Interface structure in magnetic multilayers using x-ray standing waves

Ajay Gupta,[1] Dileep Kumar,[1] and Carlo Meneghini[2]
[1]*UGC-DAE Consortium for Scientific Research, Indore - 452017, India*
[2]*Dip Di Fisica "E. Amaldi," Università di Roma Tre, I-00146 Roma, Italy*
(Received 11 September 2006; revised manuscript received 21 November 2006; published 27 February 2007)

It is demonstrated that interface structure in thin film nanostructures can be studied with a depth resolution of a fraction of a nanometer by using x-ray standing waves generated by a multilayer mirror used as a substrate. Two interfaces of a few nm thick Fe layer in magnetic trilayer structures Tb/Fe/Tb and Cr/Fe/Cr could be clearly resolved using x-ray standing waves generated by an underlying W/Si multilayer mirror. It is found that in both the cases rms roughness of the two interfaces Fe-on-Tb(Cr) and Tb(Cr)-on-Fe are not equal. For example, roughness of Fe-on-Tb interface is 1.2 nm, while that of Tb-on-Fe interface is 0.7 nm. The technique is particularly suitable in systems in which x-ray scattering contrast between adjacent layers is poor.

DOI: 10.1103/PhysRevB.75.064424 PACS number(s): 75.70.Cn, 68.65.Ac, 68.49.Uv, 61.10.Kw

I. INTRODUCTION

Magnetic multilayers have been a subject of extensive studies because of their wide-ranging applications in memory devices, read-write heads, and spintronics. Systems such as Fe/Cr, Co/Cu which exhibit giant magnetoresistance are already in use in nonvolatile memories and read-write heads, while multilayers such as Fe/Tb and Fe/Pt which exhibit perpendicular magnetic anisotropy (PMA) are strong candidates for high density recording media. In recent years there has been a growing realization that the interface structure in such multilayers strongly affects their magnetic properties.[1–4] In general the two types of interfaces in periodic multilayers, viz., A-on-B and B-on-A, are not identical. This asymmetry in the structure of the interfaces may have significant effect on the magnetic properties of the multilayer structures. For example, in Fe/V multilayers it is found that both chemical and the magnetic profiles are nonsymmetrical in the interfacial region.[5,6] Mössbauer measurements confirm that negative induced polarization takes place only at the Fe-on-V interface from the V side whereas from the Fe side at the V-on-Fe interface the Fe magnetic moments exceed the bulk value.[6] Several studies on Fe/Ag multilayer have been reported in the literature.[7–9] Schurrer *et al.* have used a monolayer of ^{57}Fe as Mössbauer probe of either Fe-on-Ag or Ag-on-Fe interfaces.[9] It is found that Fe-on-Ag interface is more diffused as compared to Ag-on-Fe interface. This difference in the structure of the two interfaces can be the cause of a difference in the average magnetic moment of Fe atoms at the two interfaces.[9] In Fe/Cr multilayers, it is found that even in epitaxial films, some interface alloying takes place.[10–15] It has been shown that the relatively small measured values for the bilinear coupling, the reversed phase of the short wavelength oscillations compared to those predicted by *ab initio* calculations, and the presence of a slowly varying exchange coupling bias are caused by interface alloying.[10–13] Numerous studies have been done to elucidate the structure of the two interfaces, and it is found that Cr-on-Fe interface is more diffused as compared to Fe-on-Cr interface.[11–16] In Fe/Tb multilayers the perpendicular magnetic anisotropy originates from the interfacial regions. Using a ^{57}Fe Mössbauer probe layer placed at either of the two interfaces, it has been inferred that Fe-on-Tb interface is more diffused as compared to the Tb-on-Fe interface.[17] Further, by eliminating one of the two interfaces by putting an Ag blocking layer, it has been shown that PMA originates mainly from the Fe-on-Tb interface.[18] Thus, it is important to elucidate the structure of the two types of interfaces in order to understand the behavior of the magnetic multilayers.

A variety of techniques such as *in situ* scanning tunneling microscopy (STM) measurements during progressive stages of deposition, Mössbauer spectroscopy with a ^{57}Fe probe layer, angle resolved Auger-electron spectroscopy (AES), low temperature nuclear orientation, or NMR have been used to characterize the interface structure.[1,7,10–15] However, as discussed later on, most of the techniques either do not have sufficient depth resolution so as to resolve the structure of the two interfaces, or may not be probing the true interfaces.

In the present work, we demonstrate that x-ray standing waves generated using a multilayer mirror can be used to resolve the structure of the two types of interfaces, i.e., A-on-B and B-on-A. Fe/Tb and Fe/Cr systems have been studied. Fe/Tb is a classic example of multilayers with perpendicular magnetic anisotropy where asymmetry of interfaces plays an important role in determining magnetic anisotropy. Fe/Cr multilayers are archetypal example of giant magnetoresistance systems, and asymmetry of interface structure in this system has been studied extensively.[11–16] In cases of both Tb/Fe/Tb and Cr/Fe/Cr trilayers deposited on top of W/Si mirrors, it is found that the two interfaces of the Fe layer namely Fe-on-Tb(Cr) and Tb(Cr)-on-Fe can be clearly resolved, providing unambiguous information about the structure of the two interfaces. Under these standing wave conditions, all the x-ray based characterization techniques such as x-ray absorption fine structure (XAFS), x-ray diffraction (XRD), and nuclear forward scattering can be used with sufficient depth resolution so as to elucidate the structure of the two interfaces separately.

Use of x-ray standing waves in the study of thin films and multilayers is well demonstrated in the literature.[19–22] In the present experiment, x-ray standing waves are generated using a W/Si multilayer mirror, which acts as a substrate for

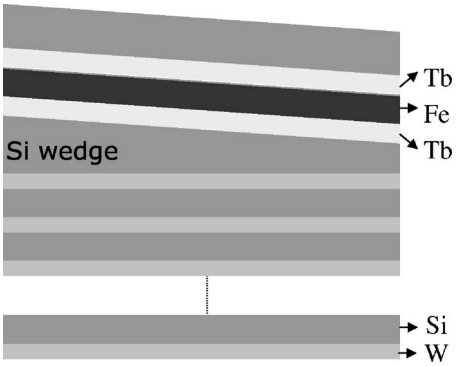

FIG. 1. Schematic of the complete multilayer structure with Tb/Fe/Tb trilayer.

the system to be studied, namely, a Tb(Cr)/Fe/Tb(Cr) trilayer. When the x rays are allowed to fall on the system at an angle around the Bragg peak of W/Si multilayer, standing waves are generated in the system, which extend beyond the mirror and into the Tb(Cr)/Fe/Tb(Cr) trilayer. Elemental concentration depth profiles are obtained by monitoring the x-ray fluorescence as the antinode is allowed to sweep across the interfaces. Separation of the two successive antinodes is equal to the bilayer periodicity of the W/Si multilayer, which also determines the depth resolution of the technique.

II. EXPERIMENTAL

The structure of the multilayers used for studying Tb/Fe/Tb trilayer, designated as Fe/Tb multilayer, is shown in Fig. 1. The mirror consists of 20 bilayers of [W 1.5 nm/Si 3.0 nm]. The last Si layer is in the form of a wedge with its thickness varying from 3.0 nm to 5.0 nm over a length of 2.0 cm. On top of this mirror a Tb 2.0 nm/Fe 3.0 nm/Tb 2.0 nm/Si 9.0 nm structure was deposited. The wedge is used in order to continuously vary the height of the Tb/Fe and Fe/Tb interfaces with respect to the standing wave pattern formed by the underlying W/Si mirror. Positions of the antinodes can also be varied by varying the angle of incidence; as the angle of incidence is varied across the width of the multilayer Bragg peak, the position of the antinode moves over the bilayer thickness.[23] An unambiguous information about the structure of the Tb-on-Fe and Fe-on-Tb interfaces is obtained by measuring x-ray fluorescence both as a function of the angle of incidence as well as distance along the length of the wedge. The multilayer structure used to study Cr/Fe/Cr trilayer, designated as Fe/Cr multilayer, consists of: [W 2.0 nm/Si 3.0 nm]$\times$10/Si 5.0 nm/Cr 2.0 nm/Fe 4.0 nm/Cr 2.0 nm/Si 5.0 nm.

The W/Si mirror was deposited on a float-glass substrate using ion-beam sputtering in a vacuum chamber with a base pressure of 1×10^{-7} mbar, while the Si_{wedge}/Tb/Fe/Tb/Si structure was deposited by electron beam evaporation in a UHV chamber with a base pressure of 1×10^{-9} mbar. Ion-beam sputtering was used to deposit the W/Si multilayer, as it is known that this technique gives more smooth interfaces and thus a higher reflectivity.[24] In the case of the Fe/Cr multilayer, the whole of the structure was deposited using ion-beam sputtering.

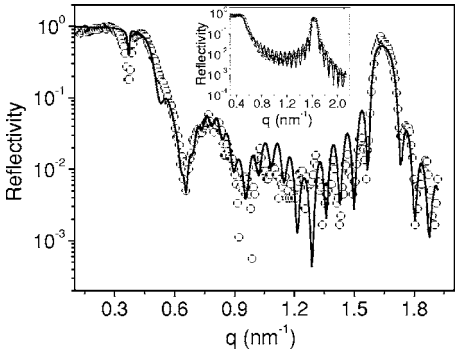

FIG. 2. Reflectivity pattern of the Fe/Tb multilayer, taken at a distance of 4.0 mm from one end of the sample. The continuous curve represents the best fit to the data. The inset shows the x-ray reflectivity pattern of the W/Si multilayer mirror, which is used as a substrate for deposition of Tb/Fe/Tb trilayer.

Simultaneous x-ray reflectivity and fluorescence measurements on Fe/Tb multilayer were done at the ID32 beamline of ESRF, Grenoble. The x-ray beam energy of 7.5 keV was selected, which lies between the *K* absorption edge of Fe and the *L* absorption edge of Tb, thus eliminating the Tb fluorescence. This simplifies the measurements. Fluorescence spectrum was measured using a Rontec XFlash detector with an energy resolution of 200 eV. In case of Fe/Cr system, reflectivity and fluorescence measurements were done using Bruker D8 diffractometer fitted with a Göbble mirror on the incident beam side in order to obtain monochromatic beam corresponding to Cu $K\alpha$ radiation. Fluorescence spectrum was measured using an Amptek model XR-100T/CR PIN diode with an energy resolution of 250 eV.

III. RESULTS

1. Fe/Tb *system*

The inset in Fig. 2 gives x-ray reflectivity of the multilayer [W 1.5 nm/Si 3.0 nm]$\times$20, which has been used as a substrate for deposition of Tb/Fe/Tb trilayer. Reflectivity data has been fitted using Parratt's formalism.[25–27] Since reflectivity is not very sensitive to the roughnesses of individual W and Si layers, the average roughness of W and Si layers was taken as a fitting parameter. The continuous curve gives the fitting of the reflectivity data yielding the multilayer structure as: [W 1.4 nm/Si 2.8 nm]$\times$20 and the average interface roughness as 0.5$\pm$0.05 nm, respectively. The parameters thus obtained have been used as input for fitting reflectivity of the complete multilayer structure. The reflectivity of the complete multilayer structure was measured at different distances from one end, corresponding to different thicknesses of the Si wedge layer. Reflectivity of the complete multilayer is dominated by that of the underlying W/Si multilayer, therefore, it is not possible to get the thickness and roughness of individual Tb, Fe, Si layers very reliably. However, the total film thickness can be obtained reliably from the period of the Kiessig oscillations. Thus, the fitting of the reflectivity was done in order to get the total thickness of the multilayer, which in turn yielded the thick-

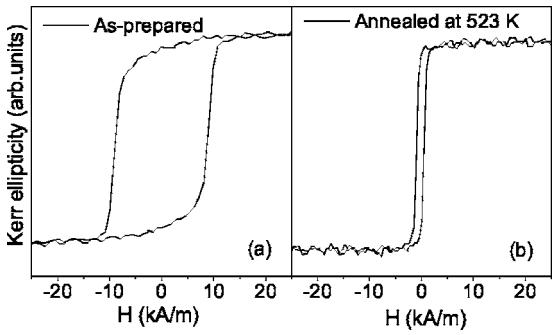

FIG. 3. The longitudinal MOKE hysteresis loops of the (a) as-prepared Fe/Tb multilayer and (b) multilayer annealed at 523 K for 60 min.

ness gradient of the wedge (the thickness of the other layers being constant) as 1.0 ± 0.05 nm/cm, in conformity with the designated value. A more detailed fitting of the reflectivity data was done simultaneously with the fluorescence data as described later on. Figure 2 shows a typical reflectivity of the complete multilayer structure taken at a distance of 4.0 mm from one end and the corresponding fitting.

The longitudinal MOKE measurements done on the as-deposited film are shown in Fig. 3. The film does not show saturation even up to a field of 25 kA/m. A remanence value of less than unity and large coercivity suggest substantial perpendicular anisotropy in the specimen. Annealing of the film at 523 K for 60 min results in a square loop with a coercivity of 800 A/m. This suggests that the perpendicular anisotropy disappears after annealing at 523 K.

The fluorescence measurements as a function of $q=4\pi\sin\theta/\lambda$, θ being the angle of incidence, were done at several positions along the length of the specimen, corresponding to different thickness of the Si wedge. Figure 4 shows the Fe fluorescence data as a function of q for three different thickness of the Si wedge layer. A prominent increase in the fluorescence is observed around the first Bragg angle of the underlying W/Si multilayer due to formation of standing waves and the resultant enhancement of the x-ray intensity inside the multilayer. One may note that the fluorescence spectrum consist of two rather broad overlapping peaks.

The fluorescence intensity at any given value of q is obtained by integrating the concentration profile $\rho(z)$ of Fe layer weighted with the x-ray intensity $I(q,z)$ at that depth

$$F(q) \propto \int I(q,z)\rho(z)dz, \tag{1}$$

$I(q,z)$ is obtained as the square of the magnitude of the total field $E_j(r)$ at a point $\mathbf{r}$ in the layer j (as shown in Fig. 5), which is the sum of that of the transmitted and reflected waves[23]

$$E_j(r) = E_j^t(r) + E_j^r(r), \tag{2}$$

where,

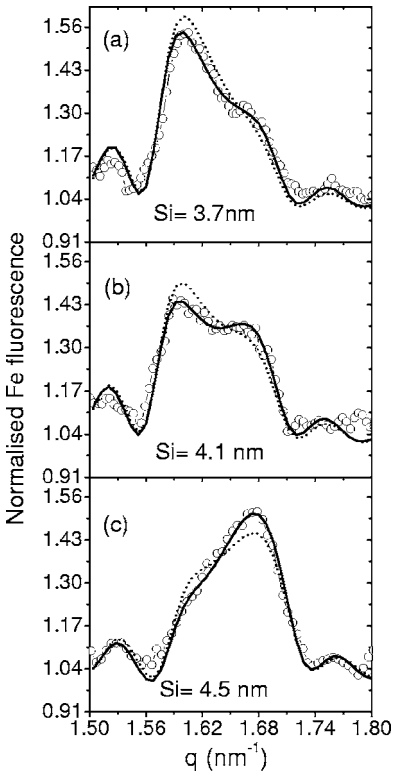

FIG. 4. The Fe fluorescence data from the Fe/Tb multilayer for three different thickness of the Si wedge layer. The continuous curves represent the simultaneous fit to the three data sets. The best fit is obtained with roughness of Tb-on-Fe interface $\sigma_{\mathrm{Tb/Fe}}=0.7$ nm and that of Fe-on-Tb interface $\sigma_{\mathrm{Fe/Tb}}=1.2$ nm. For comparison, the dotted curve represents the simulated fluorescence pattern taking the roughness of both the interfaces equal to 0.95 nm.

$$E_j^t(r) = E_j^t(0)\exp(-ik_{j,z}z)\exp[i(\omega t - k_{j,x}x)], \tag{3}$$

and

$$E_j^r(r) = E_j^r(0)\exp(+ik_{j,z}z)\exp[i(\omega t - k_{j,x}x)]. \tag{4}$$

The transmitted and reflected components at the top of the jth layer $E_j^t(0)$ and $E_j^r(0)$ can be calculated using the recursion relations[25,27]

$$E_j^r = a_j^2 X_j E_j^t, \tag{5}$$

$$E_{j+1}^t = \frac{a_j E_j^t T_j}{1 + a_{j+1}^2 X_{j+1} R_j} \tag{6}$$

with

$$X_j = \frac{(R_j + a_{j+1}^2 X_{j+1})}{1 + a_{j+1}^2 X_{j+1} R_j} \tag{7}$$

and

$$a_j = \exp(-ik_{j,z}d_j),$$

d_j and k_j being the thickness and wave vector of x rays in the jth layer. The complex transmition and reflection coefficient

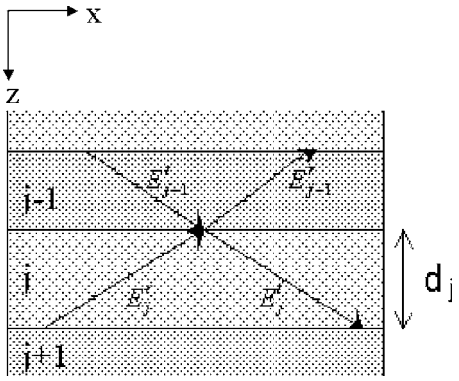

FIG. 5. The schematic ray diagram of x-rays inside the multilayer.

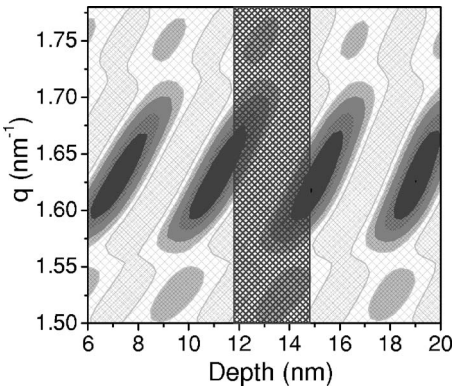

FIG. 6. The contour plot of the x-ray intensity distribution inside the Fe/Tb multilayer as a function of q. The position of the Fe layer is shown as shaded bar.

from the interface between layer j and $j+1$, having a rms roughness of σ_j are given as

$$T_j = \left(\frac{2k_{j,z}}{k_{j,z}+k_{j+1,z}}\right)\exp[\sigma_j^2(k_{j,z}-k_{j+1,z})^2/2], \tag{8}$$

and

$$R_j = \left(\frac{k_{j,z}-k_{j+1,z}}{k_{j,z}+k_{j+1,z}}\right)\exp[-2\sigma_j^2 k_{j,z}k_{j+1,z}]. \tag{9}$$

X-ray intensity inside the multilayer, $I(q,z)$ has been calculated as a function of q and z, using Eqs. (2)–(9) and is shown in Fig. 6 as a contour plot. The position of the Fe layer is marked as a shaded bar. Figure 6 can be used to understand the origin of the two peaks in the Fe fluorescence data. One may note that as q increases and spans the width of the Bragg peak, various antinodes move across the bilayer thickness of the underlying W/Si multilayer. For $q \approx 1.61$ nm^{-1}, rth antinode partly overlaps with the Fe-on-Tb interface of the Fe layer, giving rise to the first peak in the fluorescence. With increasing q this antinode moves out of the Fe layer thus resulting in a decrease in the fluorescence intensity. However, as the q is increased further, $(r+1)$th antinode moves inside and partially overlaps with the Tb-on-Fe interface giving rise to the second peak.

It is important to note that while the rth antinode moves across the Fe-on-Tb interface the $(r+1)$th antinode moves across the Tb-on-Fe interface. Therefore, the shape of the first peak in the fluorescence depends upon the Fe concentration variation across the Fe-on-Tb interface, while the shape of the second peak depends upon the Fe concentration profile across the Tb-on-Fe interface. As the thickness of the Si wedge increases, the Tb/Fe/Tb trilayer moves upward with respect to the field distribution that is essentially determined by the underlying W/Si multilayer structure. This upward movement of the Fe layer reduces the overlap of the rth antinode with Fe layer, at the same time increasing the overlap of $(r+1)$th antinode. Thus, with increasing thickness of the wedge, intensity of the first peak in the fluorescence comes down while that of the second peak builds up. A detailed fitting of the fluorescence data can unambiguously yield the roughnesses of the two interfaces separately. The parameters which primarily influence the Fe fluorescence curve are, (i) bilayer periodicity and interface roughnesses of the underlying W/Si multilayer (which is determined independently from the fitting of the reflectivity of the W/Si multilayer alone), (ii) height of the Fe layer relative to the top of the W/Si multilayer, (iii) thickness of the Fe layer and roughnesses of its two interfaces. In fact, the reflectivity and Fe fluorescence at the three positions (i.e., six data sets) were fitted simultaneously with the height of the Fe layer, its thickness and the two interface roughness $\sigma_{\mathrm{Fe/Tb}}$ and $\sigma_{\mathrm{Tb/Fe}}$ taken as fitting parameters. The best fit to the fluorescence data, shown by the continuous curves, is obtained with the roughness of Tb-on-Fe interface $\sigma_{\mathrm{Tb/Fe}}$ being equal to 0.7 ± 0.1 nm and that of Fe-on-Tb interface $\sigma_{\mathrm{Fe/Tb}}$ equal to 1.2 ± 0.1 nm, and the thickness of the Fe layer being equal to 3.0 ± 0.1 nm. The fact that all three fluorescence patterns show very good fit with the same set of parameters, lends confidence to the values of fitted parameters. It may be noted that, since the thin film deposition is well calibrated, the thickness of the Fe layer as well as the wedge are known before hand with good accuracy (the fitted values are found to be equal to the nominal values within experimental errors of ±0.1 nm). Thus, two roughness are the main fitting parameters. For comparison, the dotted curves in Fig. 6 show the simulated fluorescence curve by taking roughness of both interfaces equal to 0.95 nm, keeping all the other parameters fixed. One can note that there is a large discrepancy of this curve with the experimental data, demonstrating the sensitivity of the technique.

2. Fe/Cr *system*

Figures 7(a) and 7(b) gives the x-ray reflectivity and fluorescence of the multilayer [W 2.0 nm/Si 3.0 nm]$\times$10/Si 5.0 nm/Cr 2.0 nm/Fe 4.0 nm/Cr 2.0 nm/Si 5.0 nm. The actual structure of the W/Si multilayer alone, as determined from the reflectivity is [W 2.1 nm/Si 3.1 nm]$\times$10. The structure of the complete multilayer as obtained from the simultaneous fitting of the reflectivity and fluorescence data is found to be [W 2.1 nm/Si 3.1 nm]$\times$10/Si 5.2 nm/Cr 2.1 nm/Fe 4.0 nm/Cr 2.1 nm/Si 5.0 nm. The best fit of the fluorescence data gives the interface roughness values of $\sigma_{\mathrm{Fe/Cr}}=0.7\pm0.1$ nm and $\sigma_{\mathrm{Cr/Fe}}=1.1\pm0.1$ nm. For comparison

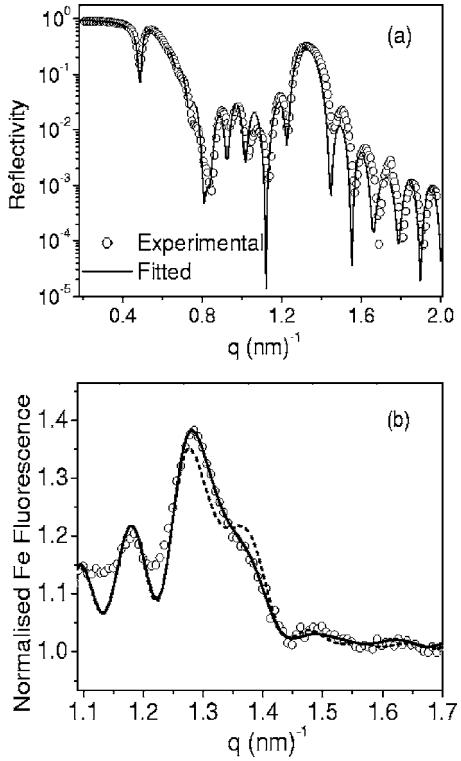

FIG. 7. (a) X-ray reflectivity and (b) Fe-fluorescence of the Fe/Cr multilayer. The continuous curve, which represents the best fit to the data corresponds to roughness values of $\sigma_{Cr/Fe}=1.1$ nm and $\sigma_{Fe/Cr}=0.7$ nm. For comparison, the dashed curve represents the simulated fluorescence pattern taking the roughness of both the interfaces equal to 0.9 nm.

the simulated fluorescence for $\sigma_{Fe/Cr}=\sigma_{Cr/Fe}=0.9$ nm is also shown with the dotted curve. There is a clear disagreement of this simulated curve with the experimental data. These results show that Cr-on-Fe interface is rougher as compared to the Fe-on-Cr interface.

IV. DISCUSSIONS

In the literature, a variety of techniques such as *in situ* STM,[11–13] conversion electron Mössbauer spectroscopy (CEMS),[14,17] angle resolved AES (Ref. 10) etc., have been used in order to resolve the structure of the two interfaces in magnetic multilayers. *In situ* STM measurements during growth of the Fe/Cr multilayer itself have been used to study the structure of the surface of the layers of the two elements.[11–13] However, this work has been criticized on the grounds that the STM image of a free surface during intermediate stages of growth may not represent the structure of the subsequently formed interface, as a significant interdiffusion will modify the interface structure. The CEMS has been widely used to differentiate between the two interfaces of Fe/M (M=Cr, Tb, V, Ag, etc.) multilayer by depositing a probe layer of ^{57}Fe either at Fe-on-M or at M-on-Fe interface. However, a redistribution of ^{57}Fe atoms during deposition of subsequent layers may obscure the information from a given depth at which the ^{57}Fe marker layer was deposited.

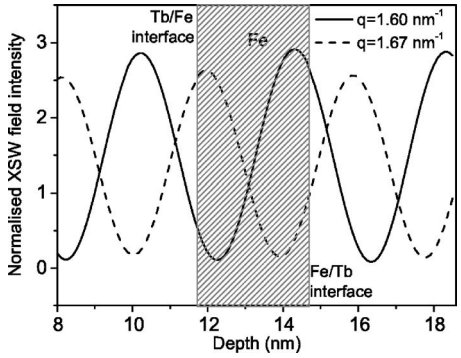

FIG. 8. Simulated standing wave field intensity inside the Fe/Tb multilayer structure at two different q values (1.60 nm^{-1} and 1.67 nm^{-1}) corresponding to the two peaks in the Fe fluorescence.

Uzdin[15] *et al.* have argued that the observed difference in the Mössbauer spectra obtained with the ^{57}Fe probe at the Fe-on-Cr and Cr-on-Fe interfaces in a Fe/Cr multilayer can be understood in terms of an algorithm for interface alloying which includes ballistic deposition with consequent rising up of some atoms on the surface. According to this model, the asymmetry in the interdiffusion at the two interfaces, as inferred from the difference in the hyperfine field distribution of a thin ^{57}Fe marker layer at the two interfaces, may be just an artifact of the technique used. ^{57}Fe marker layer has also been used to elucidate the asymmetry of interfaces in Fe/Tb multilayers,[17] however this result may also be subjected to a similar criticism. In contrast to these earlier works, the present technique based on x-ray standing wave provides a direct and unambiguous information about the roughness of the two interfaces in a single specimen.

Figure 8 gives the simulated field intensity inside the multilayer at two q values corresponding to the two peaks in the fluorescence pattern. It may be noted that there is a large contrast in the x-ray intensity at the two interfaces of the Fe layer. Thus, by doing XAFS or nuclear forward scattering measurements at these two q values, one can get depth selective information about the two interfaces. It may be noted that large intensity contrast between the positions of nodes and antinodes comes because of a large scattering contrast between the W and Si layers, and is independent of the scattering contrast between the layers under study (e.g., Fe/Cr or Fe/Tb). Thus, the technique is particularly suitable in systems in which x-ray scattering contrast between adjacent layers is poor.

V. CONCLUSIONS

It is demonstrated that x-ray standing waves generated using periodic multilayers can clearly resolve the two interfaces of a few nm thick Fe layer. Studies on Tb/Fe/Tb trilayer show that the Tb-on-Fe interface is smoother than the Fe-on-Tb interface. In the case of the Cr/Fe/Cr system, Fe-on-Cr interface is smoother. Such characterization of interface structure in magnetic multilayers is important as their magnetic properties are significantly affected by roughness

of the individual interfaces. The technique is particularly suitable in systems in which x-ray scattering contrast between adjacent layers is poor. X-ray based characterization techniques such as, XAFS or nuclear forward scattering measurements in such structures, with appropriately chosen values of scattering vector q, can give detailed atomic as well as magnetic structure of the two interfaces in the same sample.

ACKNOWLEDGMENTS

The authors wish to thank Tien-Lin Lee for help in doing the measurements at ID32 beamline of ESRF, Grenoble, and to Satish Potdar for help in the sample preparation. Financial support from the Indo-French Center for Promotion of Advanced Research is gratefully acknowledged. One of the authors (D.K.) would like to thank the Council for Scientific and Industrial Research, India for financial support.

[1] J. Lu, P. L. Kuhns, M. J. R. Hoch, W. G. Moulton, and A. P. Reyes, Phys. Rev. B **72**, 054401 (2005).
[2] V. F. Los, Phys. Rev. B **72**, 115441 (2005).
[3] A. Cole, B. J. Hickey, T. P. A. Hase, J. D. R. Buchanan, and B. K. Tanner, J. Phys.: Condens. Matter **16**, 1197 (2004).
[4] D. Olligs, D. E. Burgler, Y. G. Wang, E. Kentzinger, U. Rucker, R. Schreiber, T. Bruckel, and P. Grunberg, Europhys. Lett. **59**, 458 (2002).
[5] H. Fritzsche, Y. T. Liu, J. Hauschild, and H. Maletta, Phys. Rev. B **70**, 214406 (2004).
[6] V. M. Uzdin and L. Häggström, Phys. Rev. B **72**, 024407 (2005).
[7] T. Phalet, M. J. Prandolini, W. D. Brewer, P. Schuurmans, N. Severijns, B. G. Turrell, B. Vereecke, and S. Versyck, Phys. Rev. B **71**, 144431 (2005).
[8] P. J. Schurer, C. Zelinski, and B. Heinrich, Phys. Rev. B **48**, 2577 (1993).
[9] P. J. Schurer, C. Zelinski, and B. Heinrich, Phys. Rev. B **51**, 2506 (1995).
[10] B. Heinrich, J. F. Cochran, D. Venus, K. Totland, D. Atlan, S. Govorkov, and K. Myrtle, J. Appl. Phys. **79**, 4518 (1996).
[11] A. Davies, A. J. Stroscio, D. T. Pierce, and R. J Celotta, Phys. Rev. Lett. **76**, 4175 (1996).
[12] Y. J. Choi, I. C. Jeong, J.-Y. Park, S.-J. Kahng, J. Lee, and Y. Kuk, Phys. Rev. B **59**, 10918 (1999).
[13] C. M. Schmidt, D. E. Bürgler, D. M. Schaller, F. Meisinger, H.-J. Güntherodt, and K. Temst, J. Appl. Phys. **89**, 181 (2001).
[14] M. Kubik, T. Slezak, M. Przybylski, W. Karas, and J. Korecki, Vacuum **63**, 337 (2001); T. Shinjo and W. Keune, J. Magn. Magn. Mater. **200**, 598 (1999).
[15] V. Uzdin, W. Keune, and M. Walterfang, J. Magn. Magn. Mater. **240**, 504 (2002).
[16] A. Gupta, A. Paul, M. Gupta, C. Meneghini, U. Pietsch, K. Mibu, A. Maddalena, S. D. Toe, and G. Principi, J. Magn. Magn. Mater. **272**, 1219 (2004).
[17] B. Scholz, R. A. Brand, and W. Keune, Phys. Rev. B **50**, 2537 (1994); F. Richomme, B. Scholz, R. A. Brand, W. Keune and J. Teillet, J. Magn. Magn. Mater. **156**, 195 (1996).
[18] W. S. Kim, W. Kleemann, J. Tappert, and W. Keune, J. Appl. Phys. **84**, 4384 (1998).
[19] M. J. Bedzyk, G. M. Bommarito, M. Caffrey, and T. L. Penner, Science **248**, 52 (1990); Y. L. Qian *et al.*, *ibid.* **265**, 1555 (1994); A. Kazimirov *et al.*, *ibid.* **282**, 930 (1998).
[20] B. N. Dev, A. K. Das, S. Dev, D. W. Schubert, M. Stamm, and G. Materlike, Phys. Rev. B **61**, 8462 (2000); S. K. Ghose, B. N. Dev, and A. Gupta, *ibid.* **64**, 233403 (2001).
[21] S. K. Kim and J. B. Kortright, Phys. Rev. Lett. **86**, 1347 (2001); S. H. Yang, N. Mannella, S. K. Kim, J. B. Kortright, J. Underwood, F. Salmassi, E. Arenholz, A. Young, Z. Hussain, M. A. Van Hove, and C. S. Fadley, J. Phys.: Condens. Matter **14**, 407 (2002).
[22] A. Gupta, P. Rajput, A. Saraiya, V. R. Reddy, M. Gupta, S. Bernstorff, and H. Amenitsch, Phys. Rev. B **72**, 075436 (2005).
[23] S. K. Ghose and B. N. Dev, Phys. Rev. B **63**, 245409 (2001).
[24] M. Gupta, A. Gupta, D. M. Phase, S. M. Chaudhari, and B. A. Dasannacharya, Appl. Surf. Sci. **205**, 309 (2003).
[25] L. G. Parratt, Phys. Rev. **95**, 359 (1954).
[26] http://www.hmi.de/bensc/instrumentation/instrumente/v6/refl/parratt_en.htm.
[27] D. K. G. de Boer, Phys. Rev. B **44**, 498 (1991).